LARGE EDDY SIMULATION OF PULSED BUOYANT JET IN CROSSFLOW

Wit, L. de[1] & Rhee, C. van[1]
[1]*Section of Dredging Engineering, Delft University of Technology, the Netherlands*

Abstract Mixing of a continuous (unpulsed) buoyant or non buoyant jet in crossflow (JICF) have been studied extensively, both experimentally and numerically [6, 2, 1]. Sometimes the jet flow is non constant in time but pulsed at a certain frequency. This pulsing can influence mixing. Some publications can be found about pulsed non-buoyant JICF [3, 4]. To our knowledge there is no literature on pulsed buoyant JICF. The aim of present work is to share Large Eddy Simulation (LES) results on the influence of pulsing at different frequencies on the buoyant JICF path, concentrations and turbulent structures.

SIMULATIONS

The simulation domain is shown in Figure 1a. Our interest is to improve simulations to determine the environmental impact of buoyant dredging sediment jets (a dredging jet is denser than the ambient) created at the keel of moving dredging vessels. Therefore a schematised dredging vessel is included in the domain by a direct forcing immersed boundary method. An important environmental factor is the amount of the buoyant dredging jet which can be found near the water surface behind the dredger. Therefore we focus on the jet concentrations behind the aft of the dredging vessel at $x = 100D$. Special attention is paid to the jet material which, against gravity and initial vertical momentum, ends up above the keel ($z < 0$ in the coordinate system of Figure 1a). From observations and measurements at a dredging vessel we know that the jet inflow can fluctuate strongly around $St = fD/w_{j0} = 0.18$. In the simulations of this paper the jet inflow velocity is pulsed by a sine function with amplitude w_{j0}; the inflow varies between 0 and $2w_{j0}$. The frequency of pulsing varies to obtain $0.07 < St < 0.27$. For all simulations the initial jet has a velocity ratio $\gamma = \sqrt{\frac{\rho_{j0} w_{j0}^2}{\rho_{cf} u_{cf}^2}} = 1.28$, Richardson number $Ri = 1.08$ and $Re = 4800$, all based on the time averaged jet velocity w_{j0}. The LES code is second order accurate in time and space and uses a staggered scheme [5]. The WALE sgs model is used with $Cs = 0.325$. Both crossflow and jet inflow velocity are prescribed by laminar profiles without turbulent fluctuations. The computational grid consists of 32 million cells with 10 cells acros D at outflow and 30-80 cells across the bend over jet at $x > 5D$.

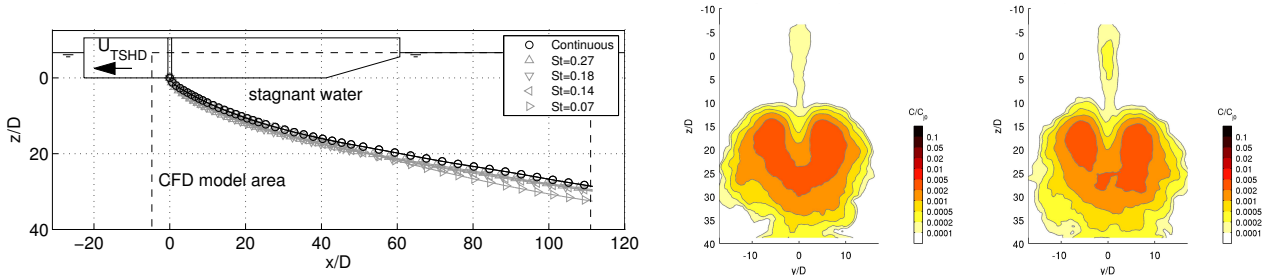

(a) (b) (c)

Figure 1. Computational set up buoyant JICF with simulated paths (a), jet concentration at $x = 100D$ continuous run (b), pulsed St=0.27 (c).

RESULTS

Figure 1a shows that the paths of pulsed buoyant JICF deviate only slightly from the continuous buoyant JICF. For $0.27 < St < 0.07$ the jet penetrades up to $4D$ deeper at $x = 100D$. The jet concentration profiles at $x = 100D$ in Figure 1b-c show the familiar kidney shaped concentration contours caused by the counter rotating vortex pair. Both the unpulsed and the pulsed buoyant JICF in Figure 1b-c have a narrow zone of jet material outside the main kidney shaped jet body which extends to $z < 0$ all the way up to the water surface. For the pulsed buoyant JICF the jet concentration inside this narrow zone is larger than for the unpulsed buoyant JICF. Table 1 summarises some jet concentration results at $x = 100D$ for all pulsed runs. It makes clear that the maximum jet concentration inside the main jet is decreased 13-25% by pulsing, in other words: pulsing enhances mixing. On the other hand is the amount of material at $z < 0$ not necessarily larger for pulsed runs: only $St = 0.27$ show increased percentages of material at $z < 0$. The maximum jet concentration at $z < 0$ however, is 16-50% larger for all pulsed runs compared to the continuous run. From Table 1 can be seen that even at a large distance downstream of $x = 100D$ pulsing has some impact on jet concentrations, but the influence of

Table 1. Pulsed buoyant JICF results at $x = 100D$.

run	C_{max}/C_{j0} at $z < 0$	Percentage material $z < 0$	$C_{max/C_{j0}}$ inside main jet
Continuous	$1.8 \cdot 10^{-4}$	0.59%	$4.1 \cdot 10^{-3}$
St=0.27	$2.7 \cdot 10^{-4}$	0.71%	$3.6 \cdot 10^{-3}$
St=0.18	$2.4 \cdot 10^{-4}$	0.53%	$3.7 \cdot 10^{-3}$
St=0.14	$2.1 \cdot 10^{-4}$	0.43%	$3.7 \cdot 10^{-3}$
St=0.07	$2.4 \cdot 10^{-4}$	0.57%	$3.1 \cdot 10^{-3}$

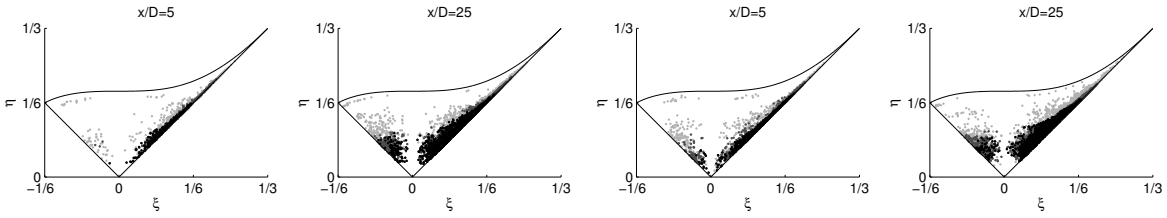

(a) (b)

Figure 2. Lumley triangle pulsed and non-pulsed buoyant JICF. a) continuous, b) St=0.27 (1Hz). The color of the dots represents the location inside the buoyant jet: black is the core $> 0.5C_{max}$, dark grey is $> 0.1C_{max}$, light grey is $> 0.01C_{max}$. C_{max} is the maximum jet concentration in that particular cross section. More results in final manuscript.

pulsing is not that large that it completely alters the buoyant JICF concentration outcomes. The influence is largest for the highest St number (highest pulsing frequency). Although the percentage of material near the surface at $z < 0$ is small (less than 1%), the concentrations at $z < 0$ of the order $10^{-4}C_{j0}$ are still relevant from environmental perspective and the impact of pulsing on these concentrations is substantial.

Energy spectra inside the pulsed and non-pulsed buoyant JICF show a large peak in each spectrum with higher harmonics at 2,4 and 8 times the pulsing frequency, Figure in final manuscript.

The Lumley triangle of a non-pulsed buoyant JICF in Figure 2a shows most points at the right edge of the triangle when $x = 5D$: the turbulence inside the buoyant jet starts rod-like (axisymmetric with one large eigenvalue of the stress tensor). For larger distances downstream $x = 25D, x = 50D, x = 100D$ ($x = 50D, x = 100D$ will be shown in full manuscript) more points are found on the left side (disk-like turbulence, axisymmetric with one small eigenvalue) and the points scatter at all possible values along the η axis which means that there are both locations with almost isotropic turbulence ($\eta = 0$) and with very non-isotropic turbulence ($\eta >>$). The locations at the core (black dots) are closer to the origin of the Lumley triangle and therefore have more isotropic turbulence than the locations at the edges. The pulsed buoyant JICF in Figure 2b shows the same behaviour as the unpulsed one at $x = 25D, x = 50D, x = 100D$ ($x = 50D, x = 100D$ will be shown in full manuscript). But at $x = 5D$ the pulsed buoyant JICF shows more locations on the left edge: close to the origin turbulence inside the pulsed buoyant JICF is more disk-like and less rod-like than the unpulsed buoyant JICF.

More results and analysis in the final manuscript.

CONCLUSIONS

In final manuscript.

References

[1] J. Andreopoulos and W. Rodi. Experimental investigation of jets in a crossflow. *J. Fluid Mech.*, **138**:93–127, 1984.

[2] V.H. Chu and M.B. Goldberg. Buoyant forced plumes in crossflow. *Journal of Hydraulic Division*, **100**(9):1203–1214, 1974. ASCE.

[3] Frank Muldoon and Sumanta Acharya. Direct numerical simulation of pulsed jets-in-crossflow. *Computers and Fluids*, **39**(10):1745 – 1773, 2010.

[4] R. T. MâĂŹCLOSKEY, J. M. KING, L. CORTELEZZI, and A. R. KARAGOZIAN. The actively controlled jet in crossflow. *Journal of Fluid Mechanics*, **452**:325–335.

[5] L. de Wit and C. van Rhee. Testing different advection schemes for coarse high re les simulations of jet in crossflow and coflow. *Proceedings of ETMM9*, 2012.

[6] J. Ziefle and L. Kleiser. Large-eddy simulation of a round jet in crossflow. *AIAA Journal*, **47**(5):1158–1172, 2009.